



Article

Pt Cluster Modified h-BN for Gas Sensing and Adsorption of Dissolved Gases in Transformer Oil: A Density Functional Theory Study

Yingang Gui ^{1,*} , Tao Li ¹, Xin He ¹, Zhuyu Ding ¹ and Pingan Yang ²

¹ College of Engineering and Technology, Southwest University, Chongqing 400715, China; litao199811@outlook.com (T.L.); lovelife824@163.com (X.H.); dingzy@swu.edu.cn (Z.D.)

² Key Laboratory of Industrial Internet of Things & Networked Control, Ministry of Education, Chongqing University of Posts and Telecommunications, Chongqing 400065, China; yangpa@cqupt.edu.cn

* Correspondence: yinganggui@swu.edu.cn

Received: 14 October 2019; Accepted: 6 December 2019; Published: 8 December 2019



Abstract: Hexagonal-Boron nitride nanotubes (h-BN) decorated with transition metals have been widely studied due to their enhanced physicochemical properties. In this paper, Pt cluster-modified h-BN is proposed as a sensitive material for a novel gas sensor for the online malfunction monitoring of oil-immersed transformers. The inner oil is ultimately decomposed to various gases during the long-term use of oil-immersed transformers. Exposure to excessively high temperatures produces the alkanes CH₄ and C₂H₆, whereas different degrees of discharge generate H₂ and C₂H₂. Therefore, the identification of H₂, CH₄, and C₂H₂ gas efficiently measures the quality of transformers. Based on the density functional theory, the most stable h-BN doped with 1–4 Pt atoms is employed to simulate its adsorption performance and response behavior to these typical gases. The adsorption energy, charge transfer, total density of states, projected density of states, and orbital theory of these adsorption systems are analyzed and the results show high consistency. The adsorption ability for these decomposition components are ordered as follows: C₂H₂ > H₂ > CH₄. Pt cluster-modified h-BN shows good sensitivity to C₂H₂, H₂, with decreasing conductivity in each system, but is insensitive to CH₄ due to its weak physical sorption. The conductivity change of Pt_n-h-BN is considerably larger upon H₂ than that upon C₂H₂, but is negligible upon CH₄. Our calculations suggest that Pt cluster modified h-BN can be employed in transformers to estimate their operation status.

Keywords: Pt cluster modified h-BN; adsorption and sensing; oil dissolved gases; simulation

1. Introduction

Oil-immersed transformers are extensively employed in modern power systems. Oil-immersed transformers are recognized as one of the most essential electric equipment because of their outstanding power conversion function and universal application. However, inevitable malfunctions associated with the long-term use of transformers, such as local overheating, partial discharge, and equipment wear out, are likely to cause catastrophic damage to the entire power system. Thus, effective methods for the online monitoring of transformers have been developed by the power sector. Along with different types of faults, various impurity gases, including H₂, CH₄, C₂H₆, and C₂H₂, are generated by transformers [1–3]. Exposure to excessive temperature produces the alkanes CH₄ and C₂H₆, whereas different degrees of discharge generate H₂ and C₂H₂. Given that H₂, CH₄, and C₂H₂ are the three typical gases in transformer faults, their identification effectively measures the quality of transformers. The condition of the transformer can be speculated by analyzing the concentration of these three typical gases and the variation of conductivity in the oil. Given the good sensitivity and versatility of

gas sensors comparing with other testing methods [4], a new type of gas sensor with selectivity and sensitivity can be developed to strengthen the running stability of oil-immersed transformers.

Boron nitride nanotubes (BN), also known as white graphene, are widely employed in various fields. BN exhibits excellent performance, including heat resistance and acid-alkali resistance [5,6]. BN is an insulator with good gas adsorption performance due to its large specific surface area. BN is employed in biological and chemical fields. The mechanism of action between metal-doped BN and ozone, and the adsorption behavior of the drug metformin on BN fullerenes have been studied [7,8]. Hexagonal-BN nanotubes (h-BN) (8,0) are widely applied in gas adsorption and sensing [9–12]. Nevertheless, intrinsic h-BN exhibits a limited response to some inert gases, such as CH₄ and C₂H₂. Metal cluster modification, such as Pd, Pt, and Ni doping [2,13,14], is commonly employed to strengthen gas sensitive responsiveness. Pt is one of the most widely used modification metals and is considered in this work.

Metal-doped material on gas sensing has developed rapidly, with numerous transition metals considered. We proposed the use of Pt cluster-modified h-BN as a promising sensing material for the detection of dissolved gases in oil-immersed transformers in order to monitor the performance of transformers. Given the activity and catalytic properties of Pt, Pt cluster modification can ameliorate the chemical activity of the h-BN surface so obtaining improved adsorption. This doped structure has rarely been studied. Thus, we analyzed the best adsorption and structural stability of Pt cluster-modified h-BN doped with 1–4 Pt atoms. We then selected the optimal structures to examine the adsorption mechanism of H₂, CH₄, and C₂H₂. The mechanisms of how the Pt cluster-modified h-BN reacts with these components must be determined to allow for the preparation of sensors to detect transformer malfunctions.

2. Computational Details

The entire computations in this work were conducted based on the density functional theory (DFT) [15,16]. Spin-polarized calculations were unrestricted. The supercell periodic boundary condition was set as 20 Å × 20 Å × 8.5 Å to prevent interaction between neighboring cells [17,18]. The generalized gradient approximation was utilized for computation by Perdew Burke Ernzerhof for the approximation treatment of exchange-correlation functional, which is widely used in the calculation of extensive materials and their surfaces [19–21]. The Brillouin-zone was carried out by the Monkhorst-Pack scheme with the k-point set to 3 × 3 × 1, which presents good approximation for h-BN [22,23]. The double numerical plus polarization was selected as the atomic orbital basis set, whereas the DFT semi-core pseudopotential method was applied considering the relativistic effect of transition elements [24]. The energy tolerance accuracy, maximum force, and displacement were selected as 10^{−5} Ha, 2 × 10^{−3} Ha/Å, and 5 × 10^{−3} Å, respectively [25,26]. For the stationary electronic structure, a precise convergence criterion of 1.0 × 10^{−6} Ha for self-consistent field tolerance was employed [27].

We optimized the geometry of the H₂, C₂H₂, and CH₄ in oil, as well as the majorization treatment of the intrinsic h-BN structure. Pt cluster modification was considered to obtain improved adsorption performance. In this work, all possible Pt cluster-modified h-BNs doped with 1–4 Pt atoms were optimized. The best performance and the most stable structure with different Pt cluster decorations was obtained by calculating the adsorption energy (E_d) of doped fabric, and is defined in Equation (1), combined with the specific bond length and collection shape.

$$E_d = E_{Pt_n/h-BN} - E_{h-BN} - E_{Pt_n} \quad (1)$$

where n represents the number of doping atoms and E_d expresses the energy released during binding. To analyze the mechanism and effect of the adsorption process, we calculated the charge transfer (Q_t) and adsorption energy (E_{ads}) based on Equations (2) and (3).

$$Q_t = Q_1 - Q_2 \quad (2)$$

$$E_{\text{ads}} = E_{\text{gas/suf}} - E_{\text{gas}} - E_{\text{suf}} \quad (3)$$

where Q_t indicates the charge transfer amount from the gas molecules to the surface of Pt cluster modified h-BN through Mulliken population analysis while Q_1 and Q_2 represent the total net charge after and before gas adsorption, respectively. In Equation (3), E_{ads} represents the total energy of the gas molecules before adsorption. A negative E_{ads} indicates that the adsorption process is exothermic and spontaneous. The adsorption mechanism can greatly affect the conductivity and gas concentration of the entire system, which is beneficial to fabricate a gas sensor with selectivity and sensitivity. The electrical conductivity is related to energy gap and the change of energy gap will affect conductivity exponentially [28]. To further obtain the conductivity of the entire system, we determined the energy gap (E_g) of the molecular orbital between the highest occupied molecular orbital (HOMO) and the lowest occupied molecular orbital (LUMO), as defined in Equation (4) [29].

$$E_g = |E_{\text{LUMO}} - E_{\text{HOMO}}| \quad (4)$$

Total density of states (TDOS) and projected density of states (PDOS) in the adsorption are analyzed in detail for comprehension of the mechanism of the adsorption process.

3. Results and Discussions

3.1. Optimized Structure of Gas Molecules and Intrinsic h-BN

As shown in Figure 1, the optimized structure of gas molecules and intrinsic h-BN are presented. Both H_2 and C_2H_2 are linear gas molecules, whereas CH_4 is a three-dimensional tetrahedral structure, the H–H bond length in the H_2 molecule is 0.75 Å, given the weak atomic force and short atomic radius of the H atom. C–H bond lengths are 1.10 and 1.07 Å in CH_4 and C_2H_2 molecules. Different orbital hybridization causes slight difference in the C–H bond lengths. In the CH_4 molecule, the H–C–H bond angle is 109.39°. The symmetrical structure and four C–H bonds of the CH_4 molecule imparts its chemical stability. An h-BN with a perfect crystal structure is shown in Figure 1b. The mesh-like hexagonal structure is beneficial to the adsorption performance. The B–N bond length of 1.44 Å is appropriate for structural stability, both axial and circumferential distances are around this value. When all aspects are considered, h-BN is a suitable material for gas adsorption.

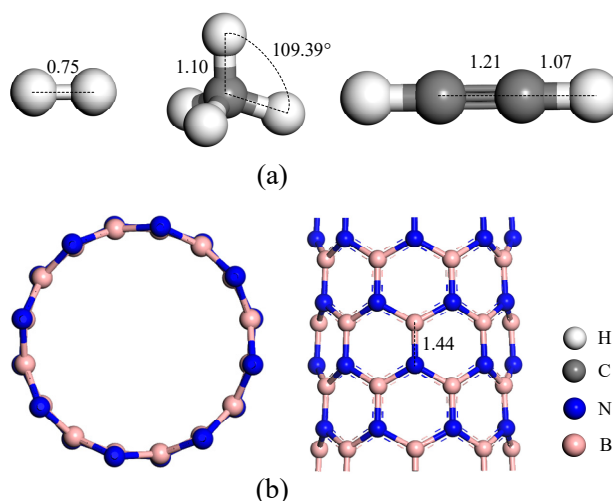


Figure 1. (a) H_2 , CH_4 , C_2H_2 molecules (b) Intrinsic hexagonal boron nitride nanotubes (h-BN).

3.2. Pt Cluster Modified h-BN

Figure 2 shows the different doping structures with 1–4 Pt atoms. The adsorption distance, charge transfer, and adsorption energy are calculated to find the most stable structures with different doping Pt atoms.

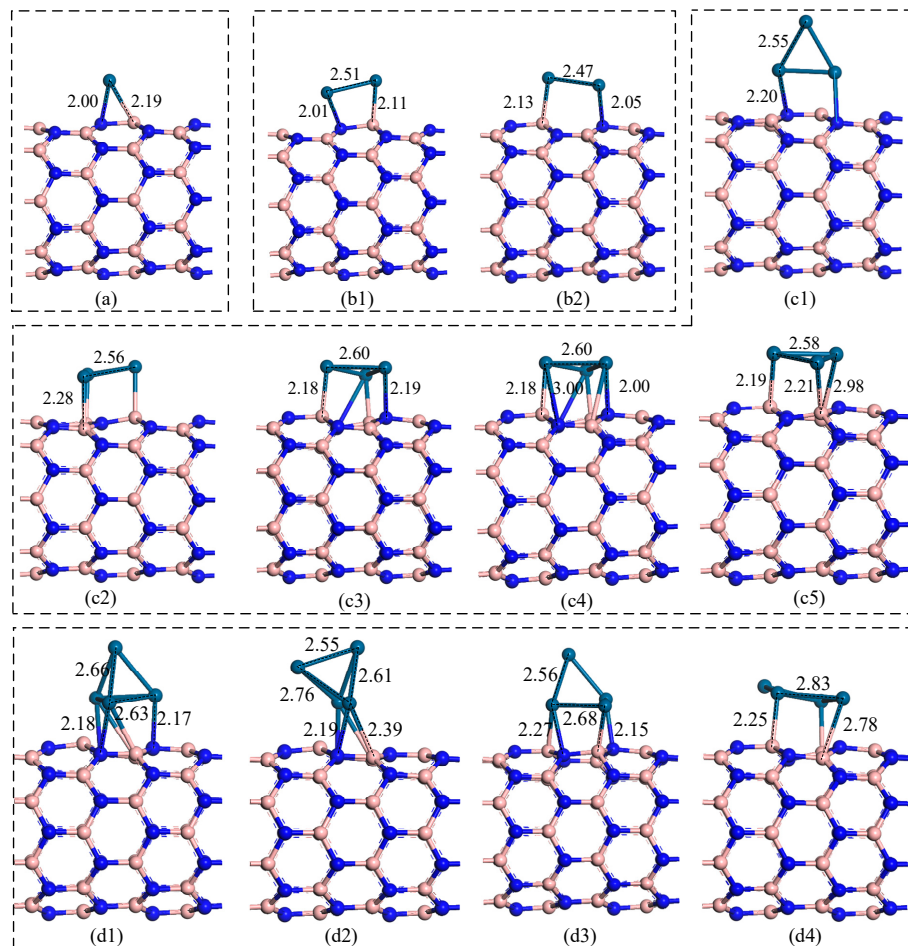


Figure 2. The structures of Pt cluster modified h-BN. The h-BN is modified by a cluster containing a Pt atom (a), two Pt atom (b1,b2), three Pt atom (c1–c5), four Pt atom (d1–d4).

Figure 2a shows the most stable structure doped with one Pt atom, which is also the only possible structure at this situation. The atomic arrangement of h-BN exhibits central symmetry and requires the location of the Pt atom to be centered. We considered different situations in the experiments. However, only the bridge site for Pt atom doping can be optimized successfully. The Pt–N bond length is 2.00 Å, which is slightly shorter than the Pt–B bond length (2.19 Å). This phenomenon illustrates the strong force between Pt and N atoms. The adsorption energy (E_d) of -1.98 eV demonstrates fine stability from the perspective of energy.

Two Pt-atom doping is also considered in this work. Different systems have been computed, as presented in Figure 2b1,b2. The two structures are the adjacent and opposite sides of the hexagon where Pt atom doping occurs. The Pt–Pt bond lengths are 2.51 and 2.47 Å, meeting the bond length between heavy metals. The E_d values of the adjacent and opposite sides are -4.83 and -4.84 eV, as shown in Figure 2b1. Dispersed Pt atoms may cause the two- and single-atom-doped structures to be similar.

As shown in Figure 2c1–c5, five possible models were generated. The clustering of the three metal atoms has been widely employed in the field of materials. Thus, the Pt₃ cluster is treated emphatically in this work to enhance gas sensitivity response. The surface structure of the intrinsic h-BN is greatly

altered after Pt₃ modification. The atom tends to protrude outward. E_d values from (c1) to (c5) are -9.02 , -8.16 , -8.31 , -8.30 , and -8.30 eV, respectively. A high E_d proves that the structure shown in Figure 2c1 exhibits stronger stability compared with the other structures.

As shown in Figure 2d1–d4, the Pt₄ cluster is employed for analysis. Many possible structures are also obtained. We finally selected the most stable structure according to the E_d and geometry structure, as shown in Figure 2d1. The adsorption energy of this structure is -12.59 eV, which is higher than that of any other structure. The three-dimensional feature also imparts stability to this structure.

To gain insight into the diversification in conductivity, we studied the band structure of systems in Figure 2a,b,c1,d1. This analysis allows for the advanced understanding of the gas adsorption mechanism. The band structure of the systems is drawn as follows:

As shown in Figure 3, the band gaps from Figure 3a–e are 3.73, 1.50, 0.30, 0.0, and 0.38 eV, respectively. The intrinsic h-BN exhibits a huge band gap of 3.73 eV, which explains the difficulty for electrons to jump from the top of the valence band to the bottom of the conduction band. This result is also consistent with h-BN being an insulator. After Pt cluster modification, the band gap in each case is greatly decreased, enhancing electrical conductivity throughout the system. After Pt₃ doping, the entire band structure is almost continuous, which may be largely due to the doping position.

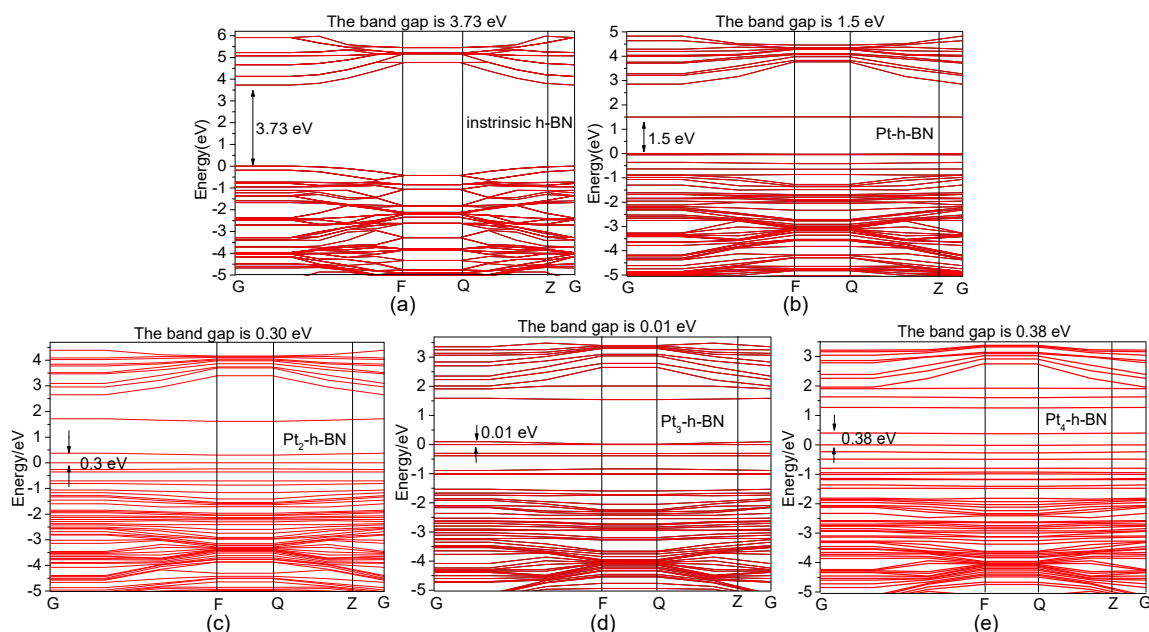


Figure 3. Energy band diagram of different structures, (a) intrinsic h-BN, (b) Pt-h-BN, (c) Pt₂-h-BN, (d) Pt₃-h-BN, (e) Pt₄-h-BN.

3.3. Adsorption of H₂, CH₄, C₂H₂ on the Surface of Intrinsic h-BN

The optimization results for the adsorption of H₂, CH₄, and C₂H₂ on intrinsic h-BN are presented in Figure 4. The geometric optimization results were calculated as the lowest energy structure according to the DFT, that is, relatively thermodynamic stability, so as to determine the adsorption energy and adsorption distance. According to the final analysis results, intrinsic h-BN exhibits low gas sensitivity response to these typical gases. The H₂, C₂H₂, and CH₄ molecular structures remain unchanged during the adsorption process, and the long adsorption distance and weak adsorption energy suggest a weak physical mechanism between gas molecules and the intrinsic h-BN. The specific parameters in the adsorption process are provided in Table 1 to further explain the adsorption performance.

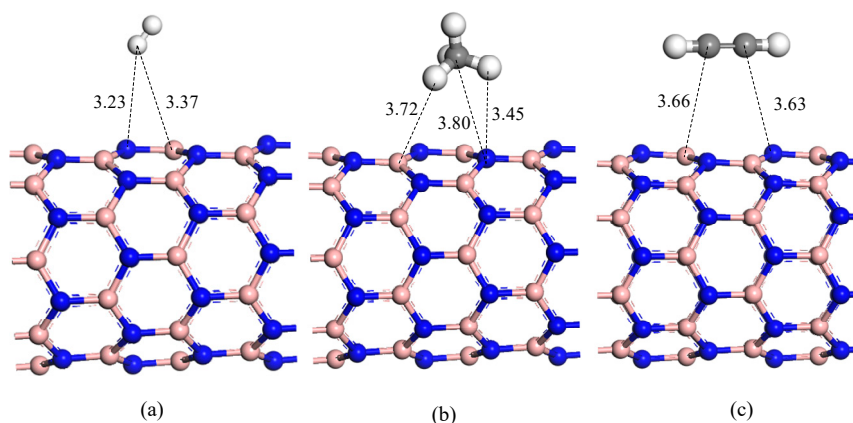


Figure 4. The structures of gas molecular adsorption on intrinsic h-BN. (a) H₂, (b) CH₄, (c) C₂H₂.

Table 1. Adsorption process parameters of adsorption of H₂, CH₄, and C₂H₂ on the surface of intrinsic h-BN.

System	Structure	Adsorption Distance (d)	Adsorption Energy (E_{ads})
H ₂ adsorption	Figure 4a	3.23 Å	−0.08 eV
CH ₄ adsorption	Figure 4b	3.45 Å	−0.06 eV
C ₂ H ₂ adsorption	Figure 4c	3.63 Å	−0.10 eV

The distance of the gas molecules to h-BN is very far, ranging from 3.23 Å to 3.63 Å, explaining the weak interaction between the molecules. The adsorption energies of H₂, CH₄, and C₂H₂ are −0.08, −0.06, and −0.10 eV, respectively. Such small adsorption energy values also correspond to the long adsorption distance. The final simulation data show that the intrinsic h-BN response to these three gases is ordered as follows: C₂H₂ > H₂ > CH₄. This order seems to be related to the characteristics of the gas molecules.

3.4. Adsorption of Gas Molecules on Pt, Pt₂ Doped h-BN

Figure 5a–f depicts the gas adsorption system on Pt- and the Pt₂-doped h-BN. The calculation parameters are shown in Table 2. Based on the optimized adsorption structure, Pt doping can improve the gas sensitivity of the entire system, especially for H₂ and C₂H₂, where strong chemical adsorption process occurs after Pt and Pt₂ doping. However, the adsorption capacity for CH₄ is insufficient, with merely weak physical and catalytic effects between the molecules. The adsorption capacity based on the simulation results is as follows: C₂H₂ > H₂ > CH₄, and the effects in all occasions are strengthened.

Figure 5a–d shows that the H–H bond is broken during the adsorption process. Two H atoms are bonded to the Pt atom at a bond length of 1.55 Å, and the adsorption energy in both cases are 1.94 and 1.97 eV. No difference is found between single- and two-atom doping due to the far distance between the H₂ molecule and the second Pt atom. After Pt atom doping, E_{ads} is increased from −0.08 eV to −1.94 eV. The rapid increase of E_{ads} with a large Q_t (0.26 e) indicates that the Pt atom can enhance the adsorption activity of the system, thereby producing a strong chemical action with the H₂ molecule.

The optimization results for CH₄ adsorption are shown in Figure 5b–e. Compared with intrinsic h-BN, the Pt- and Pt₂-doped h-BN can considerably improve the adsorption capacity, as proven by the large E_{ads} and short adsorption process distance. The bond lengths of the H atom in the CH₄ molecules to the Pt atom are 1.76 and 2.53 Å, and the molecular structure of CH₄ remains substantially unchanged. We speculate that the role between the CH₄ and Pt is biased toward physical adsorption. The structure in Figure 5e shows a weaker effect, and the stability of the doped structure causes the lower adsorption of diatomic doping compared with that of monoatomic doping.

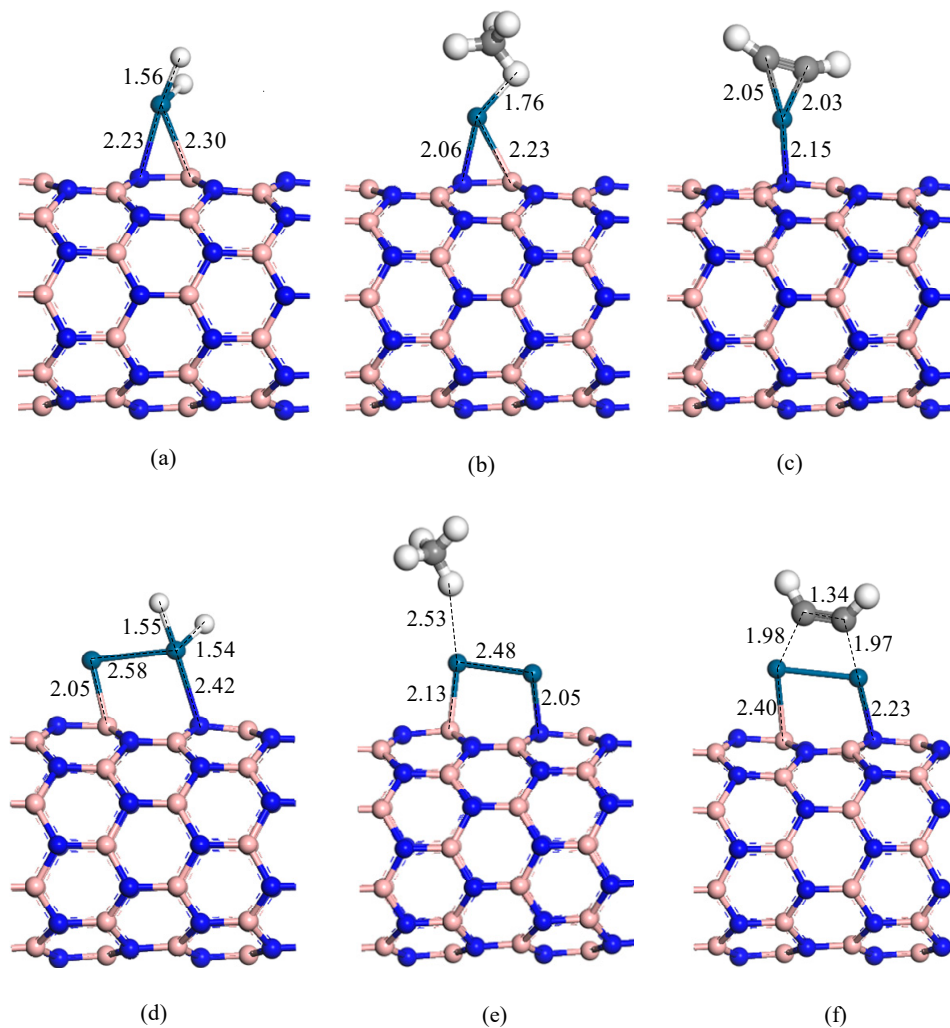


Figure 5. Adsorption of gas molecules on Pt, Pt₂ modified h-BN. (a) H₂ molecule on Pt modified h-BN, (b) CH₄ molecule on Pt modified h-BN, (c) C₂H₂ molecule on Pt modified h-BN, (d) H₂ molecule on Pt₂ modified h-BN, (e) CH₄ molecule on Pt₂ modified h-BN, (f) C₂H₂ molecule on Pt₂ modified h-BN.

Table 2. Adsorption parameters of gas molecules on Pt, Pt₂ doped h-BN: charge transfer (Q_t), adsorption distance (d), adsorption energy (E_{ads}).

System	Structure	Adsorption Distance (d)	Adsorption Energy (E_{ads})	Charge Transfer (Q_t)
H ₂ /Pt-h-BN	Figure 5a	1.56 Å	−1.94 eV	0.26 e
CH ₄ /Pt-h-BN	Figure 5b	1.76 Å	−0.97 eV	0.10 e
C ₂ H ₂ /Pt-h-BN	Figure 5c	2.03 Å	−2.60 eV	0.18 e
H ₂ /Pt ₂ -h-BN	Figure 5d	1.54 Å	−1.97 eV	0.30 e
CH ₄ /Pt ₂ -h-BN	Figure 5e	2.53 Å	−0.10 eV	0.06 e
C ₂ H ₂ /Pt ₂ -h-BN	Figure 5f	1.97 Å	−3.40 eV	0.14 e

Figure 5c–e demonstrates the large influence between C₂H₂ molecule and doped h-BN. In the single Pt atom-doped system, the Pt–B bond is fractured because of the great force, and the structure of C₂H₂ is changed from a straight line to a distorted planar structure. In the two Pt atom-doped system, the degree of distortion is evident. E_{ads} with magnitudes of 2.60 and 3.4 eV at different situations suggest a complicated process that occurs, and the adsorption effect is improved by a leap.

For improved understanding of the adsorption for manufacturing suitable gas sensors, the total density of states (TDOS), partial density of states (PDOS), and molecular orbitals for different gas adsorption scenarios were analyzed. An accurate sensor applied to the online monitoring of transformers can be implemented by identifying different parameters, including conductivity and E_g .

As shown in Figure 6a–f, the TDOS is changed after gas adsorption, and Figure 6a1–f1 presents the PDOS of corresponding situations. The adsorption of different gases shows varying effects on the TDOS. The conductivity of the entire system can be precisely modified through TDOS analysis. Finally, a sensitive gas sensor can be fabricated by analyzing the resistance value of the system. PDOS was calculated to explore advanced adsorption mechanisms, particularly the mechanism of intermolecular chemical bonding. A combination analysis can provide accurate simulation data applied to gas sensor manufacturing.

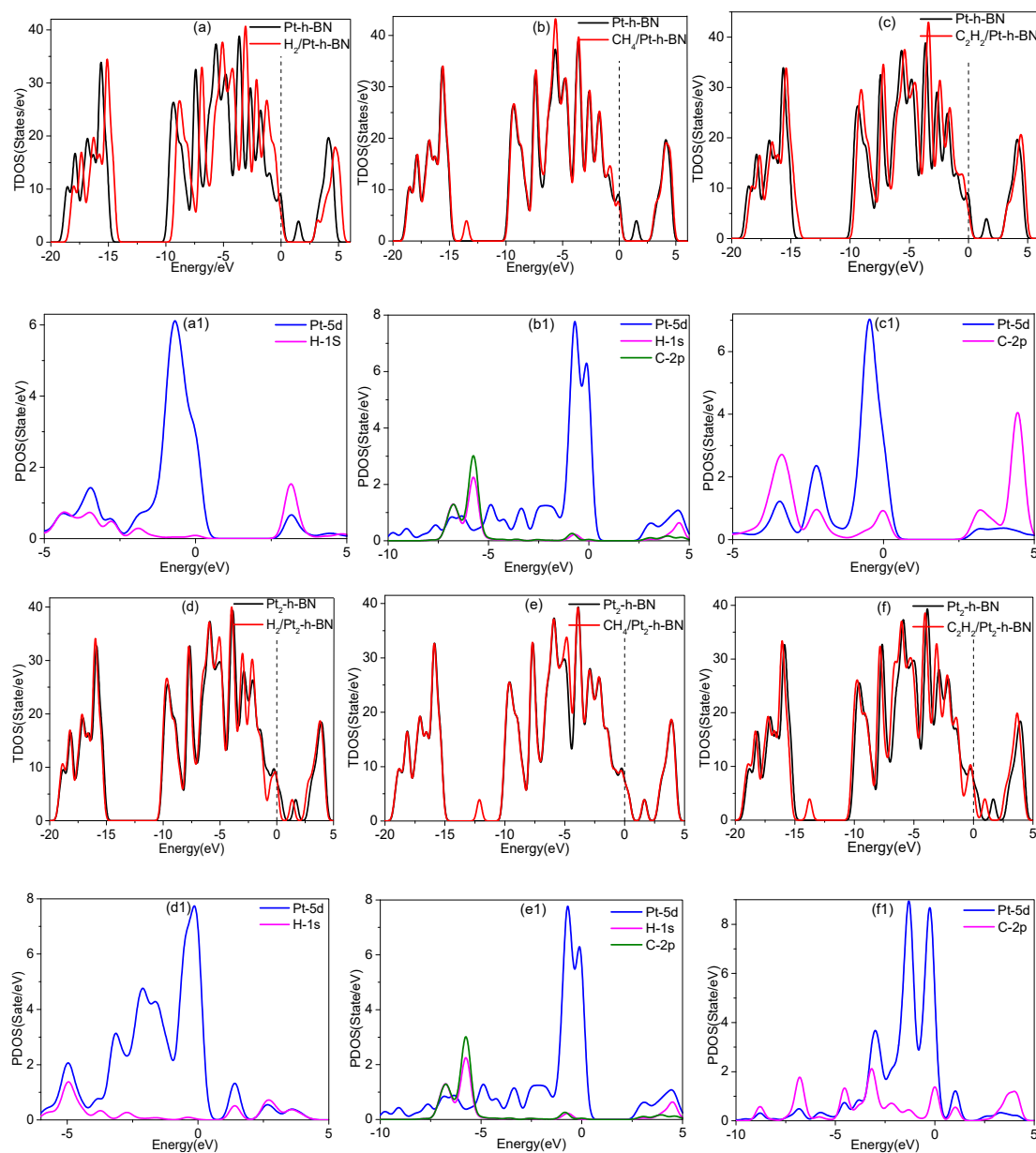


Figure 6. Total density of states (TDOS) and partial density of states (PDOS) of adsorption of gas molecules on Pt, Pt₂ modified h-BN. (a) TDOS of H₂ on Pt modified h-BN, (b) TDOS of CH₄ on Pt modified h-BN, (c) TDOS of C₂H₂ on Pt modified h-BN, (d) TDOS of H₂ on Pt₂ modified h-BN, (e) TDOS of CH₄ on Pt₂ modified h-BN, (f) TDOS of C₂H₂ on Pt₂ modified h-BN. (a1) to (f1) are PDOS of the corresponding subgraph.

In TDOS, both H₂ and C₂H₂ show remarkable changes in TDOS, but the change in CH₄ is not evident. In a single-atom-doped system, TDOS is approximately equal to 0 eV between the conduction band and the valence band, reflecting the decline in conductivity. However, the occurrence of this

phenomenon is minimal in the two-atom-doped system, because two-Pt-atoms doping increases the conductivity of the system. As shown in Figure 1a, TDOS moves to the right as a whole and then drops slightly at the right side of the Fermi level. This result indicates the reduced number of electronic fillings of the conduction band. Furthermore, the conductive property of the structure is decreased, the reason for which can be analyzed from the distribution of PDOS. Considerable orbital hybridization exists in the 5d orbital of Pt and the 1s orbital of H, which is related to the formation of Pt–H bond in the adsorption structure. Strong chemical action decreases conductivity, but this effect is minimal in the two Pt atoms doping system.

In the TDOS and PDOS of CH₄ adsorption, no considerable change is found, as shown in Figure 7b–e. Therefore, the electrical conductivity of the entire system remains unchanged. The 2p orbital of C is mainly distributed between –7.5 and –5 eV. Therefore, the effect on the entire energy band structure is minimal, as demonstrated by the weak physical function and small E_{ads} (0.97 and 0.1 eV). Such feature can be used to study new types of sensors with selectivity.

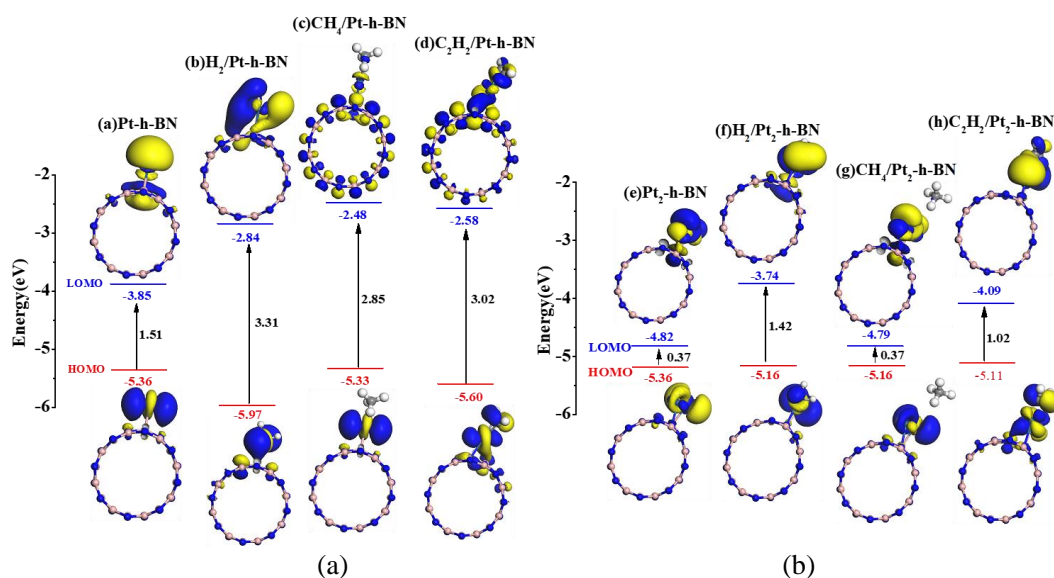


Figure 7. Molecular orbital before and after gas adsorption. (a) Pt-h-BN system, (b) Pt₂-h-BN system.

The same analytical method was used to analyze the adsorption of C₂H₂. The Pt 5d and C 2p orbitals show simultaneous peaks at the same energy level. The orbital hybridization illustrates the strong interaction between the Pt and C atoms, and the high effect between these atoms also reduces the distribution of TDOS around the Fermi level. Thus, the conductivity of the entire system will also decrease.

Frontier molecular orbital theory was analyzed for different systems, and the effect can be obtained based on the electronic behavior of Pt- and Pt₂-doped h-BN in the presence of gas molecules. Determining the features that can be practically modified will be helpful for the exploitation of gas sensors. Based on molecular orbital theory, we calculated the HOMO and LUMO distributions of the adsorption system, as shown in Figure 7. We also calculated E_g to evaluate conductivity changes, as presented in Table 3. HOMO and LUMO are mostly located near the Pt atom doping site, which is associated with the good conductivity and insulation properties of h-BN. After gas adsorption, the LUMO position is drastically changed, whereas the HOMO is slightly altered. As shown in Figure 7a–d, the 1.51 eV E_g of Pt-h-BN reflects good conductivity. When the gas molecules are close to h-BN, E_g is rapidly increased to >2.8 eV. As gas molecules transfer charge to the h-BN system, many LUMOs are on the surface of the gas molecules. In the H₂ molecule model, E_g can be remarkably improved, and a strong chemical adsorption process occurs, greatly reducing the conductivity of the entire system. Based on the comparison of different situations, almost no HOMO and LUMO distribution occurs on

the CH₄ molecules, and weak physical effects cannot largely change the conductivity. The contribution of C₂H₂ to the conductivity is slightly lesser than that of H₂. Thus, the conductivity of the entire system is slightly higher than that of the H₂ adsorption system. Figure 7e–h show that the HOMO and LUMO distribution of the gas molecule/Pt₂-h-BN system presents a similar situation. CH₄ exhibits a minor role, and E_g remains unchanged. In general, the molecular adsorption of H₂ shows the largest influence on conductivity, whereas that of CH₄ exhibits nearly no effect on conductivity.

Table 3. Molecular orbitals and energy gaps of individual molecules before and after adsorption.

Adsorption system	Structure	E_{HOMO} (eV)	E_{LUMO} (eV)	E_g (eV)
Pt-h-BN	Figure 7a	−5.34	−3.85	1.51
H ₂ /Pt-h-BN	Figure 7b	−5.97	−2.84	3.31
CH ₄ /Pt-h-BN	Figure 7c	−5.33	−2.48	2.85
C ₂ H ₂ /Pt-h-BN	Figure 7d	−5.60	−2.58	3.02
Pt ₂ -h-BN	Figure 7e	−5.19	−4.82	0.37
H ₂ /Pt ₂ -h-BN	Figure 7f	−5.16	−3.74	1.42
CH ₄ /Pt ₂ -h-BN	Figure 7g	−5.16	−4.79	0.37
C ₂ H ₂ /Pt ₂ -h-BN	Figure 7h	−5.11	−4.09	1.02

In summary, for different adsorption scenarios, conductivity decreases at varying degrees. H₂ molecular adsorption exhibits the greatest influence on conductivity, followed by C₂H₂ adsorption. CH₄ molecule adsorption is very weak, minimally contributing to conductivity. The estimated final conductivity is arranged as follows: CH₄ adsorption system > C₂H₂ adsorption system > H₂ adsorption system.

3.5. Adsorption of Gas Molecules on Pt₃, Pt₄ Doped h-BN

The gas adsorption system on Pt₃- and Pt₄-doped h-BN is depicted in Figure 8a–f. Table 4 shows very similar results between Pt- and Pt₂-doped h-BN systems. Doping structures with more modified Pt atoms are more responsive to H₂ and C₂H₂ than to CH₄, and the adsorption process with the CH₄ molecule is very weak. Drastic changes in the charge transfer amount occur at different situations. Different doping structures were compared, and the results are presented as follows.

In the H₂ adsorption system, a strong chemical adsorption process exists between Pt₃- or Pt₄-doped structure and the H₂ molecule, the adsorption energy slightly decreasing from −1.97 eV to −1.67 eV. Different degrees of adsorption process mechanism cause large changes in Q_t . In the H₂/Pt₃-h-BN system, such a large Q_t indicates that the H atom acquires numerous electrons. Therefore, great changes in conductivity exist.

In the CH₄ adsorption model, the adsorption distance of approximately 2.30 Å and adsorption energy of <1 eV greatly reflect the weak physical effects, which is consistent with previous conclusions. In the system of C₂H₂/Pt₃- and Pt₄-doped h-BN, E_{ads} of 2.16 and 2.88 eV are approaching that of the C₂H₂/Pt- and Pt₂-doped h-BN systems. This result illustrates that E_{ads} remains unchanged, and only slight differences in conductivity occurs.

The TDOS and PDOS of gas molecule adsorption on Pt₃- and Pt₄-doped h-BN are presented in Figure 9. When three Pt atoms are doping, TDOS is decreased rapidly at the Fermi level, and the TDOS to the right of the Fermi level is increased, indicating increased electronic filling conduction band. The band gap of Pt₃-h-BN is 0.01 eV, which reflects very good electrical conductivity. Additional impurity bands and chemical action worsens the conductivity. Figure 9b,c shows a spike at −5 eV, which is caused by the hybridization of the C-2p orbit and Pt-5d orbit from the PDOS. In C₂H₂ adsorption, the C-2p and Pt-5d orbits show strong hybridization at many energy levels. Strong molecular forces exhibit a great effect between the two atoms. Thus, the C₂H₂ molecule undergoes a great bend.

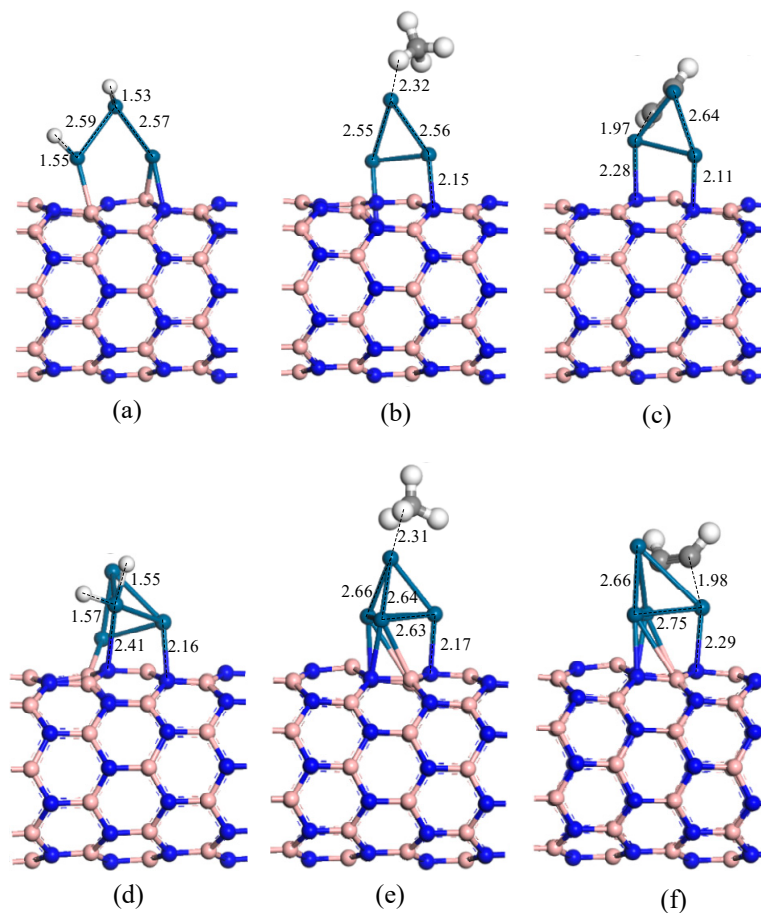


Figure 8. Adsorption of gas molecules on Pt₃, Pt₄ doped h-BN. (a) H₂ molecule on Pt₃ modified h-BN, (b) CH₄ molecule on Pt₃ modified h-BN, (c) C₂H₂ molecule on Pt₃ modified h-BN, (d) H₂ molecule on Pt₄ modified h-BN, (e) CH₄ molecule on Pt₄ modified h-BN, (f) C₂H₂ molecule on Pt₄ modified h-BN.

Table 4. Adsorption parameters of gas molecules on Pt₃, Pt₄ doped h-BN: charge transfer (Q_t), adsorption distance (d), adsorption energy (E_{ads}).

System	Structure	Adsorption Distance (d)	Adsorption Energy (E_{ads})	Charge Transfer (Q_t)
H ₂ /Pt ₃ -h-BN	Figure 8a	1.53 Å	1.67 eV	0.20 e
CH ₄ /Pt ₃ -h-BN	Figure 8b	2.32 Å	0.56 eV	0.21 e
C ₂ H ₂ /Pt ₃ -h-BN	Figure 8c	1.97 Å	2.16 eV	0.25 e
H ₂ /Pt ₄ -h-BN	Figure 8d	1.55 Å	1.58 eV	0.22 e
CH ₄ /Pt ₄ -h-BN	Figure 8e	2.31 Å	0.10 eV	0.05 e
C ₂ H ₂ /Pt ₄ -h-BN	Figure 8f	1.98 Å	2.88 eV	0.28 e

The overall change of TDOS in the Pt₄-h-BN adsorption system is relatively weak, as shown in Figure 9d–f. Only the adsorption of the H₂ gas molecule changes the TDOS at the Fermi level, and a low TDOS decreases the conductivity in this situation. As shown in Figure 9e, almost no change occurs in TDOS around the Fermi level, indicating that the CH₄ molecule contributes slightly to conductivity. The PDOS from –2.5 eV to 2.5 eV in this case is also a good illustration of this phenomenon. Almost no electronic filling is expected in the Pt atom. Only the Pt doping changes the band structure. Therefore, the conductivity does not change substantially after CH₄ adsorption. The results in Figure 9f–f1 are almost identical to the previous analysis of C₂H₂. Extraordinary orbit hybridizations occur between the C-2p and Pt-5d orbits, but the change in conductivity may be small due to the weak change around the Fermi level.

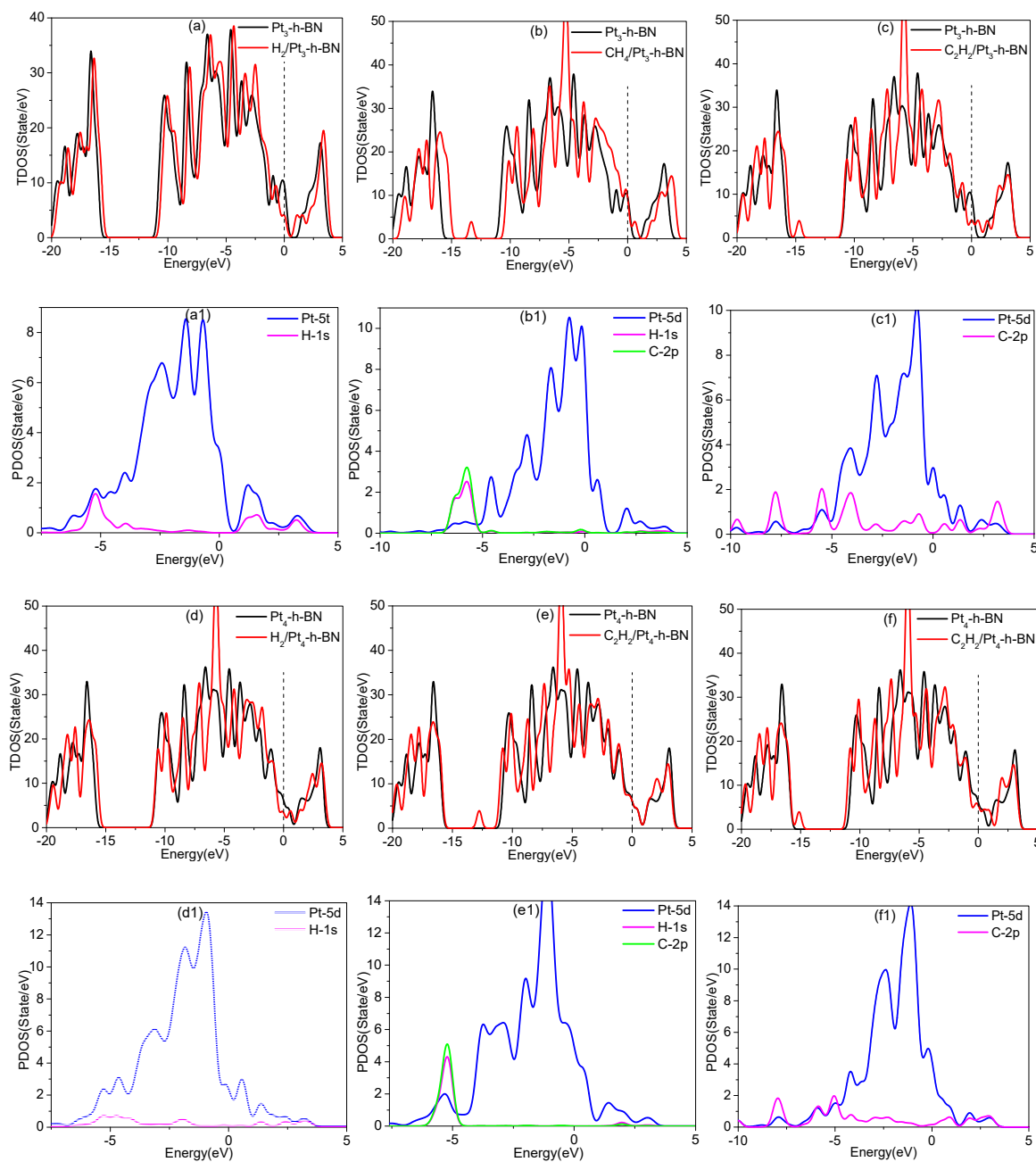


Figure 9. TDOS and PDOS of adsorption of gas molecules on Pt₃, Pt₄ modified h-BN. (a) TDOS of H₂ on Pt₃ modified h-BN, (b) TDOS of CH₄ on Pt₃ modified h-BN, (c) TDOS of C₂H₂ on Pt₃ modified h-BN, (d) TDOS of H₂ on Pt₄ modified h-BN, (e) TDOS of CH₄ on Pt₄ modified h-BN, (f) TDOS of C₂H₂ on Pt₄ modified h-BN. (a1) to (f1) are PDOS of the corresponding subgraph.

Based on the molecular orbital theory, the HOMO and LUMO distributions of the adsorbed structures were determined using the same formula. Figure 10 shows an intuitive graphical distribution, and Table 5 lists the arranged data.

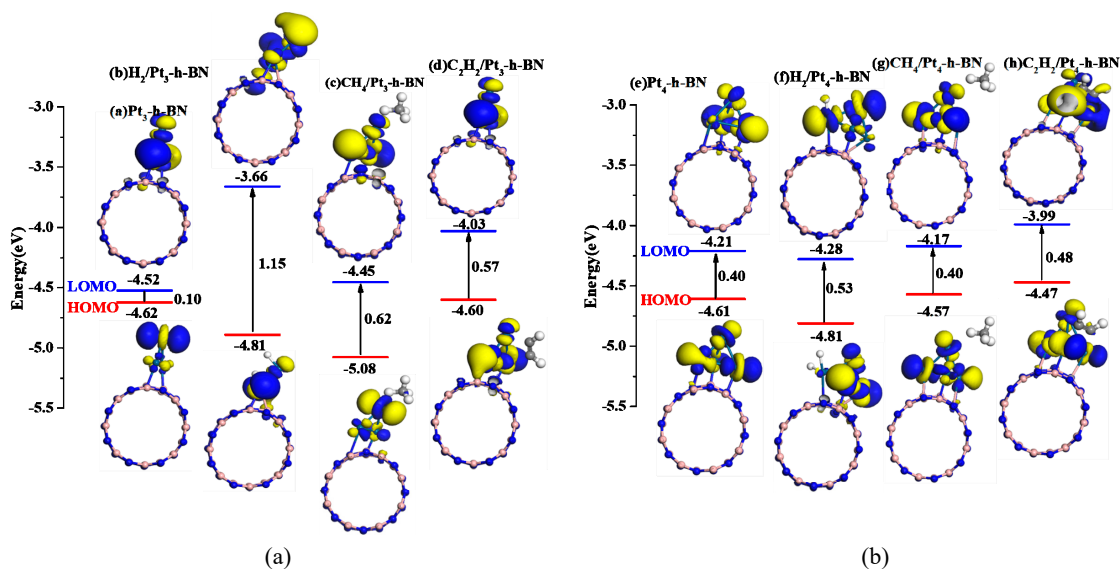


Figure 10. Molecular orbital before and after gas adsorption. (a) Pt₃-h-BN system, (b) Pt₄-h-BN system.

Table 5. Molecular orbitals and energy gaps of individual molecules before and after adsorption.

Adsorption System	Structure	E_{HOMO} (eV)	E_{LUMO} (eV)	E_g (eV)
Pt ₃ -h-BN	Figure 10a	−4.62	−4.52	0.10
H ₂ /Pt ₃ -h-BN	Figure 10b	−4.81	−3.66	1.15
CH ₄ /Pt ₃ -h-BN	Figure 10c	−5.08	−4.45	0.63
C ₂ H ₂ /Pt ₃ -h-BN	Figure 10d	−4.60	−4.03	0.57
Pt ₄ -h-BN	Figure 10e	−4.61	−4.21	0.40
H ₂ /Pt ₄ -h-BN	Figure 10f	−4.81	−4.28	0.53
CH ₄ /Pt ₄ -h-BN	Figure 10g	−4.57	−4.17	0.40
C ₂ H ₂ /Pt ₄ -h-BN	Figure 10h	−4.47	−3.99	0.48

As shown in Figure 10, E_g is decreased between HOMO and LUMO, indicating that increased metal atom doping can reduce E_g , thereby increasing the conductivity. In other respects, the contribution of gas molecules to electrical conductivity is not as remarkable as previously observed, but the degree of discrimination is still quite valuable. In general, gas adsorption can decrease the conductivity of the system, and conductivity caused by Pt₃ doping is more intense than that by Pt₄ doping.

In the Pt₃ doping system, the E_g of 0.1 eV reflects good electrical conductivity of the system. When accompanied by the adsorption of different gases, the conductivity is decreased, especially when H₂ is close to the doped structure. E_g is changed from 0.1 eV to 1.15 eV, indicating that strong adsorption with chemical bond formation decreases electrical conductivity. The role of CH₄ is non-negligible under this model, and the relatively large E_g (0.63 eV) also remarkably changes the conductivity of the system. The same effect is observed in the C₂H₂ adsorption model. Finally, we analyzed the gas/Pt₄-h-BN. As shown in Figure 10e–h, the effect of gas molecules on conductivity is slightly decreased, and no considerable changes occur after gas adsorption.

In summary. The adsorption of different molecules decreases conductivity at varying degrees. The adsorption of H₂ and CH₄ shows the greatest and weakest influence on conductivity, respectively. The final conductivity is ordered as follows: CH₄ adsorption system > C₂H₂ adsorption system > H₂ adsorption system, which is the same as that in Pt- and Pt₂-doped h-BN systems.

3.6. Comparison of Charge Transfer, Adsorption Energy, Energy Gap at Different Systems Through Table and Histogram

A comparative analysis of adsorption parameters (Q_t , E_{ads} , E_g) are carried out to present more intuitive comparison as shown in Table 6 and Figure 11. After gas molecules adsorption, Q_t is ranging

from -0.05 – $0.28 e$. It is obvious that the charge transfer amount of CH_4 is smaller than H_2 and C_2H_2 . By comparing the Q_t and E_{ads} of each adsorption systems, chemical effect occurs in H_2 , C_2H_2 , while physical effect occurs in CH_4 during the adsorption process. The adsorption ability for these decomposition components are ordered as follows: $\text{C}_2\text{H}_2 > \text{H}_2 > \text{CH}_4$. As shown in Figure 11c, E_g has different degrees of reduction after different Pt atoms modification, meaning that the conductivity of the entire system increases. When gas molecules are close to the Pt_n -h-BN, the rising E_g indicates that the conductivity of the system decrease with different degrees, H_2 and C_2H_2 molecules drastically decrease the conductivity, while CH_4 nearly does not affect electronic distribution. The final conductivity is ordered as follows: CH_4 adsorption system $> \text{C}_2\text{H}_2$ adsorption system $> \text{H}_2$ adsorption system. This work can be applied to develop new gas sensors based on the Pt cluster modified h-BN using online monitoring of the dissolved gases in transformer oil.

Table 6. Adsorption parameters summary of different systems.

Adsorption Type	Q_t (e)	E_{ads} (eV)	E_g (eV)
Pt-h-BN	/	/	1.51
Pt_2 -h-BN	/	/	0.37
Pt_3 -h-BN	/	/	0.10
Pt_4 -h-BN	/	/	0.40
H_2/Pt -h-BN	0.26	1.94	3.31
H_2/Pt_2 -h-BN	0.30	1.97	1.42
H_2/Pt_3 -h-BN	0.20	1.67	1.15
H_2/Pt_4 -h-BN	0.22	1.58	0.53
CH_4/Pt -h-BN	0.10	0.97	2.85
CH_4/Pt_2 -h-BN	0.06	0.10	0.37
CH_4/Pt_3 -h-BN	0.21	0.56	0.63
CH_4/Pt_4 -h-BN	0.05	0.10	0.40
$\text{C}_2\text{H}_2/\text{Pt}$ -h-BN	0.18	2.60	3.02
$\text{C}_2\text{H}_2/\text{Pt}_2$ -h-BN	0.14	3.40	1.02
$\text{C}_2\text{H}_2/\text{Pt}_3$ -h-BN	0.25	2.16	0.57
$\text{C}_2\text{H}_2/\text{Pt}_4$ -h-BN	0.28	2.88	0.48

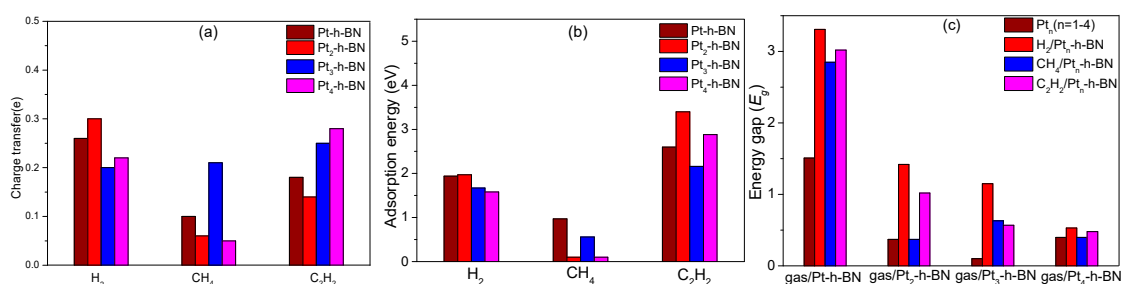


Figure 11. Contrast histogram analysis of adsorption parameters. (a) Charge transfer of all adsorption system, (b) adsorption of all adsorption system, (c) energy gap of all adsorption system.

4. Conclusions

In this study, the most stable structure of h-BN under various doping strategies is analyzed, and the Pt cluster-modified h-BN is employed to investigate its adsorbing performance on oil-decomposed components. DOS analysis and frontier molecular orbital theory are considered to comprehensively understand the interactions between gas molecules and Pt cluster-modified h-BN. A new gas sensor with selectivity and sensitivity can be developed by analyzing the responsiveness to typical gases. The specific response mechanism and conclusions are as follows:

1. Pt cluster-modified h-BN exhibits good sensitivity to C_2H_2 and H_2 due to chemical adsorption process but is insensitive to CH_4 , with only weak physical adsorption process between them.

The adsorption ability for these decomposition components occurs in the following order: $C_2H_2 > H_2 > CH_4$.

- In all doping systems, the adsorption of each gas molecule decreases the conductivity of the entire system. H_2 and C_2H_2 molecules can drastically change the conductivity, and the decreased conductivity values for C_2H_2 and H_2 are ordered as follows: $H_2 > C_2H_2$. CH_4 does not affect electronic distribution.
- In doping by different Pt atoms, the adsorption process mechanisms and adsorption are slightly different, but the good sensitivity to H_2 and C_2H_2 is consistent. On the basis of the large difference in characteristics after adsorption, Pt cluster-modified h-BN is a suitable gas sensor.

Therefore, our calculations suggest that Pt cluster-modified h-BN prepared sensors provide a facile way to practically detect transformer oil-dissolved components and can effectively estimate the operation status of transformers. Pt cluster-modified h-BN is a promising material as a gas sensor and for employment in power systems.

Author Contributions: Y.G. conceived and designed the experiments; T.L. and Y.G. performed the experiments; T.L. and P.Y. analyzed the data; Z.D. contributed analysis tools, supervision; Y.G. and Z.D. contributed funding; T.L. and X.H. proposed the methodology; P.Y. wrote the original draft; X.H. provides guidance for revise.

Funding: This work is supported by the National Natural Science Foundation of China (Grant No. 51907165), Key Laboratory of Industrial Internet of Things & Networked Control (Grant No. 2018FF04), Chongqing Research Program of Basic Research and Frontier Technology (Grant No. cstc2018jcyjAX0068).

Conflicts of Interest: The authors declare no conflict of interest.

References

- Lu, J.; Zhang, X.; Wu, X.; Dai, Z.; Zhang, J. A Ni-Doped Carbon Nanotube Sensor for Detecting Oil-Dissolved Gases in Transformers. *Sensors* **2015**, *15*, 13522–13532. [[CrossRef](#)] [[PubMed](#)]
- Zhang, X.; Hao, C.; Zhang, J.; Ju, T. Adsorption characteristic of Pd-4 cluster carbon nanotube towards transformer oil dissolved components: A simulation. *Appl. Surf. Sci.* **2017**, *419*, 802–810. [[CrossRef](#)]
- Sun, H.C.; Huang, Y.C.; Huang, C.M. A Review of Dissolved Gas Analysis in Power Transformers. *Energy Procedia* **2012**, *14*, 1220–1225. [[CrossRef](#)]
- Lee, J.H. Gas sensors using hierarchical and hollow oxide nanostructures: Overview. *Sens. Actuators B Chem.* **2009**, *140*, 319–336. [[CrossRef](#)]
- Jia, J.F.; Wu, H.S.; Jiao, H. The structure and electronic property of BN nanotube. *Phys. B Condens. Matter* **2006**, *381*, 90–95. [[CrossRef](#)]
- Bo, Z.; Huang, X.; Wen, G.; Long, X.; Yu, H.; Bai, H. Preparation and Ultraviolet-Visible Luminescence Property of Novel BN Whiskers with a Cap-Stacked Structure. *J. Phys. Chem. C* **2010**, *114*, 21165–21172.
- Farmanzadeh, D.; Askari, N. Theoretical study of ozone adsorption on the surface of Fe, Co and Ni doped boron nitride nanosheets. *Appl. Surf. Sci.* **2018**, *444*. [[CrossRef](#)]
- Anota, E.C.; Cicoletzi, H.G. GGA-based analysis of the metformin adsorption on BN nanotubes. *Phys. E Low-Dimens. Syst. Nanostruct.* **2014**, *56*, 134–140. [[CrossRef](#)]
- Xuan, Z.; Wei, C.; Zhou, Y.; Sun, W.; Ying, X. DFT simulation on H_2 adsorption over Ni-decorated defective h-BN nanosheets. *Appl. Surf. Sci.* **2018**, *439*, 246–253.
- Min, G.; Lyalin, A.; Taketsugu, T. Catalytic Activity of Au and Au₂ on the h-BN Surface: Adsorption and Activation of O₂. *J. Phys. Chem. C* **2012**, *116*, 9054–9062.
- Koch, H.P.; Laskowski, R.; Blaha, P.; Schwarz, K. Adsorption of gold atoms on the h-BN/Rh (111) nanomesh. *Phys. Rev. B Condens. Matter* **2011**, *84*, 2335–2341. [[CrossRef](#)]
- Gui, Y.; Wang, Y.; Duan, S.; Tang, C.; Zhou, Q.; Xu, L.; Zhang, X. Ab Initio Study of SOF₂ and SO₂F₂ Adsorption on Co-MoS₂. *ACS Omega* **2019**, *4*, 2517–2522. [[CrossRef](#)] [[PubMed](#)]
- Wang, Y.; Gui, Y.; Ji, C.; Tang, C.; Zhou, Q.; Li, J.; Zhang, X. Adsorption of SF₆ decomposition components on Pt₃-TiO₂(1 0 1) surface: A DFT study. *Appl. Surf. Sci.* **2018**, *459*, 242–248. [[CrossRef](#)]
- Wang, Q.; Lim, K.H.; Yang, S.W.; Yang, Y.; Chen, Y. Atomic carbon adsorption on Ni nanoclusters: A DFT study. *Theor. Chem. Acc.* **2011**, *128*, 17–24. [[CrossRef](#)]

15. Russo, T.V.; Martin, R.L.; Hay, P.J. Effective Core Potentials for DFT Calculations. *J. Phys. Chem.* **1995**, *99*, 17085–17087. [[CrossRef](#)]
16. Hensley, A.J.R.; Ghale, K.; Rieg, C.; Dang, T.; Ye, X. DFT-Based Method for More Accurate Adsorption Energies: An Adaptive Sum of Energies from RPBE and vdW Density Functionals. *J. Phys. Chem. C* **2017**, *121*, 4937–4945. [[CrossRef](#)]
17. Schultz, P.A. Local electrostatic moments and periodic boundary conditions. *Phys. Rev. B* **1998**, *60*, 1551–1554. [[CrossRef](#)]
18. Makov, G.; Payne, M.C. Periodic boundary conditions in ab initio calculations. *Phys. Rev. B Condens. Matter* **1995**, *51*, 4014. [[CrossRef](#)]
19. Li, J.; Gui, Y.; Ji, C.; Tang, C.; Zhou, Q.; Wang, Y.; Zhang, X. Theoretical study of the adsorption of SF₆ decomposition components on Ni(1 1 1) surface. *Comput. Mater. Sci.* **2018**, *152*, 248–255. [[CrossRef](#)]
20. Javid, M.A.; Khan, Z.U.; Mehmood, Z.; Nabi, A.; Hussain, F.; Imran, M.; Nadeem, M.; Anjum, N. Structural, electronic and optical properties of LiNbO₃ using GGA-PBE and TB-mBJ functionals: A DFT study. *Int. J. Mod. Phys. B* **2018**, *32*, 1850168. [[CrossRef](#)]
21. Amaya-Roncancio, S.; Linares, D.H.; Duarte, H.A.; Sapag, K. A DFT Study of Hydrogen Assisted Dissociation of CO by HCO, COH and HCOH Formation on Fe (100). *J. Phys. Chem. C* **2016**, *120*. [[CrossRef](#)]
22. Esrafil, M.D. BN co-doped graphene monolayers as promising metal-free catalysts for N₂O reduction: A DFT study. *Chem. Phys. Lett.* **2018**, *705*, 44–49. [[CrossRef](#)]
23. Froyen, S. Brillouin-zone integration by Fourier quadrature: Special points for superlattice and supercell calculations. *Phys. Rev. B Condens. Matter* **1989**, *39*, 3168–3172. [[CrossRef](#)] [[PubMed](#)]
24. Yang, Q.; Zhong, C. Understanding hydrogen adsorption in metal-organic frameworks with open metal sites: A computational study. *J. Phys. Chem. B* **2006**, *110*, 655–658. [[CrossRef](#)]
25. Gui, Y.; Chao, T.; Qu, Z.; Xu, L.; Zhao, Z.; Zhang, X. The sensing mechanism of N-doped SWCNTs toward SF₆ decomposition products: A first-principle study. *Appl. Surf. Sci.* **2018**, *440*, 846–852. [[CrossRef](#)]
26. Huo, C.F.; Ren, J.; Li, Y.W.; Wang, J.G.; Jiao, H.J. CO dissociation on clean and hydrogen precovered Fe(111) surfaces. *J. Catal.* **2007**, *249*, 174–184. [[CrossRef](#)]
27. Motl, P.M.; Tohline, J.E.; Frank, J. Numerical Methods for the Simulation of Dynamical Mass Transfer in Binaries. *Astrophys. J. Suppl* **2001**, *138*, 121. [[CrossRef](#)]
28. He, X.; Gui, Y.; Xie, J.; Liu, X.; Wang, Q.; Tang, C. A DFT study of dissolved gas (C₂H₂, H₂, CH₄) detection in oil on CuO-modified BNNT. *Appl. Surf. Sci.* **2020**, *500*. [[CrossRef](#)]
29. Hariharan, P.C.; Pople, J.A. The influence of polarization functions on molecular orbital hydrogenation energies. *Theor. Chim. Acta* **1973**, *28*, 213–222. [[CrossRef](#)]



© 2019 by the authors. Licensee MDPI, Basel, Switzerland. This article is an open access article distributed under the terms and conditions of the Creative Commons Attribution (CC BY) license (<http://creativecommons.org/licenses/by/4.0/>).